REC1 – Recognizing Off-line Flowcharts by Reconstructing Strokes and Using On-line Recognition Techniques

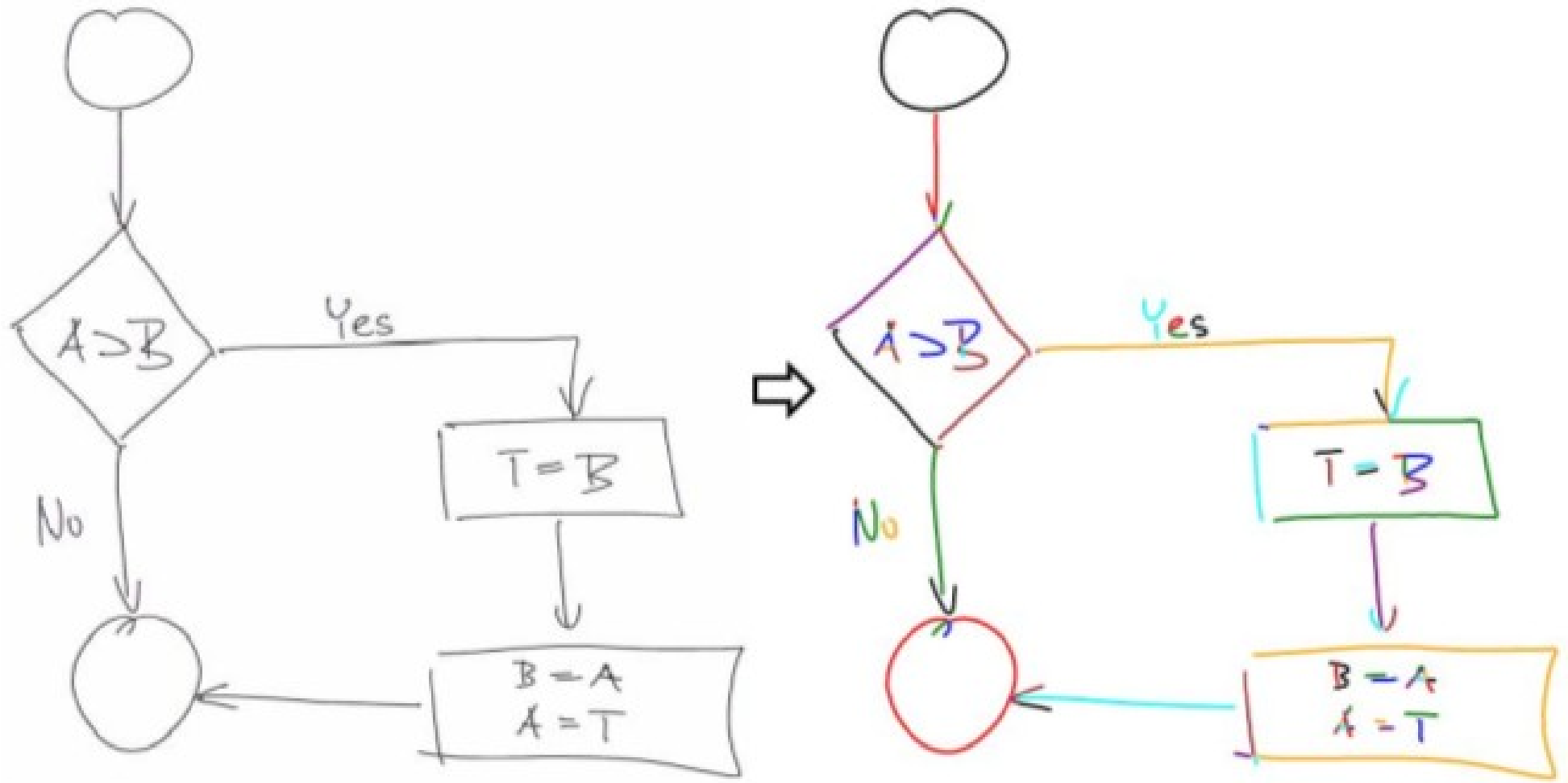

REC2 – Line-of-Sight Stroke Graphs and Parzen Shape Context Features for Handwritten Math Formula Representation

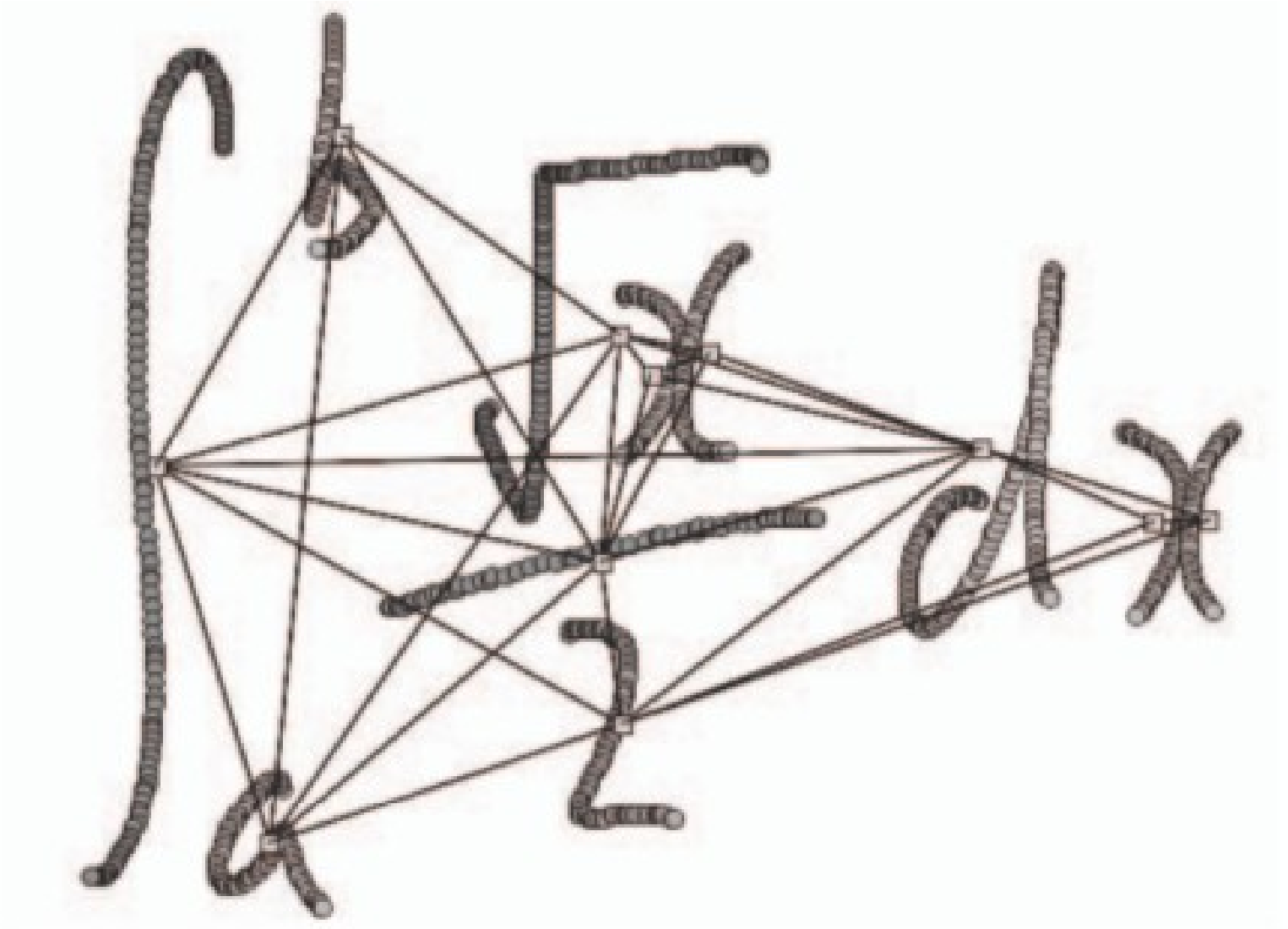

MOD1 – Robust Output Modeling in Bag-of-Features HMMs for Handwriting Recognition

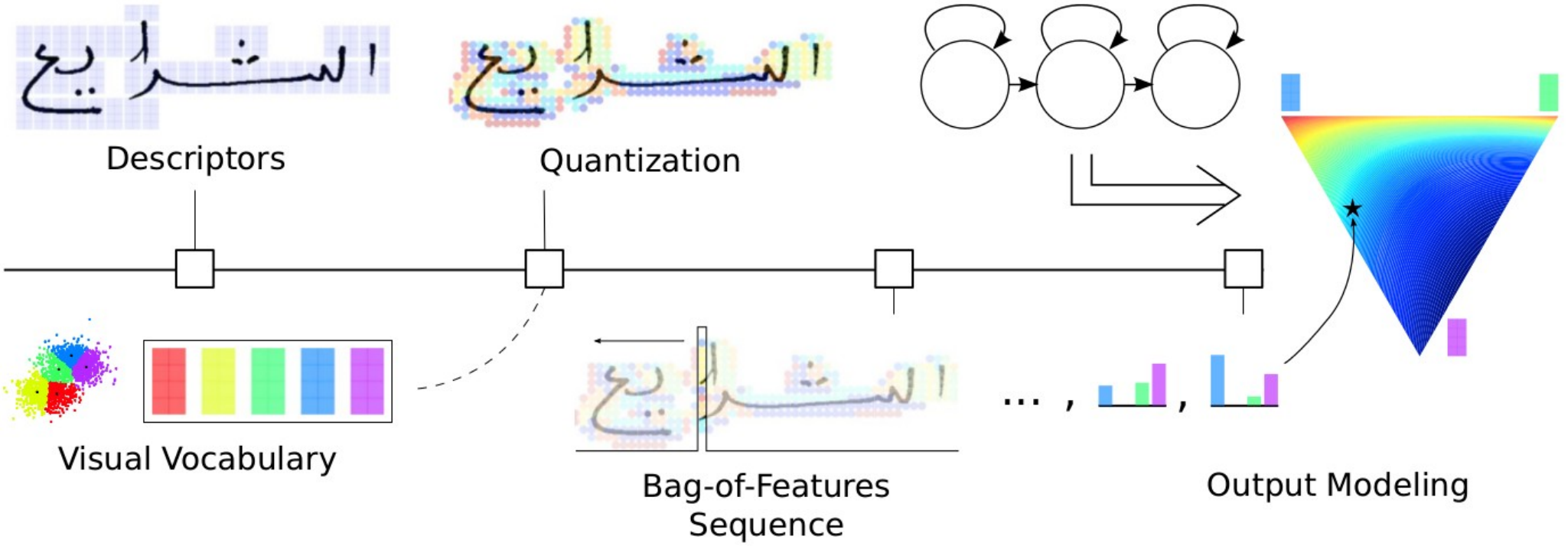

MOD2 – Line Segmentation Approach for Ancient Palm Leaf Manuscripts using Competitive Learning Algorithm

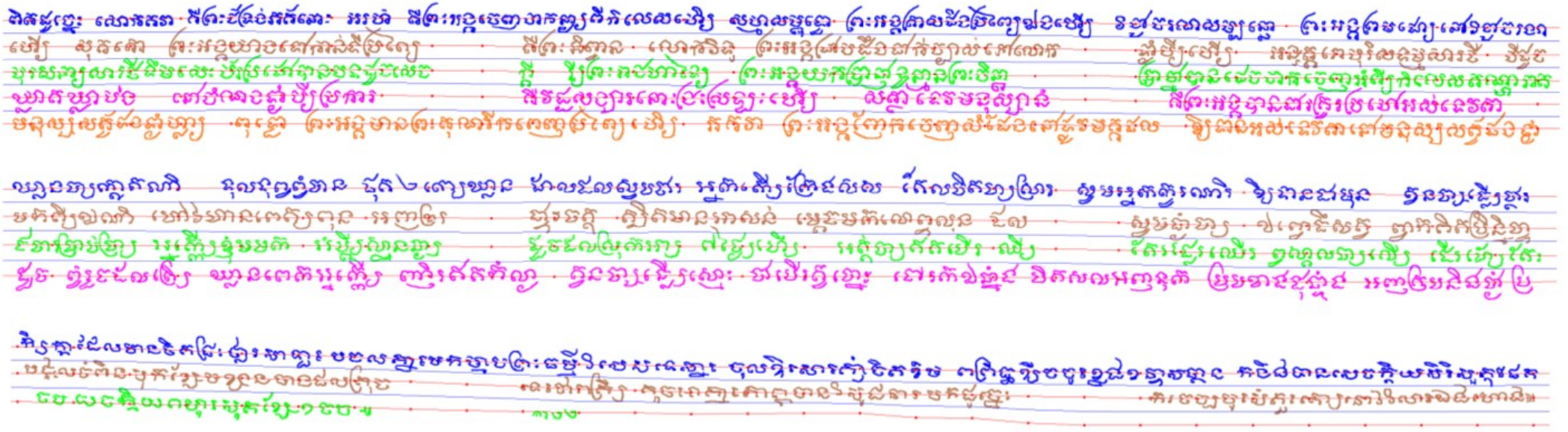

LG1 – Efficient edge-aware surface mesh reconstruction for urban scenes

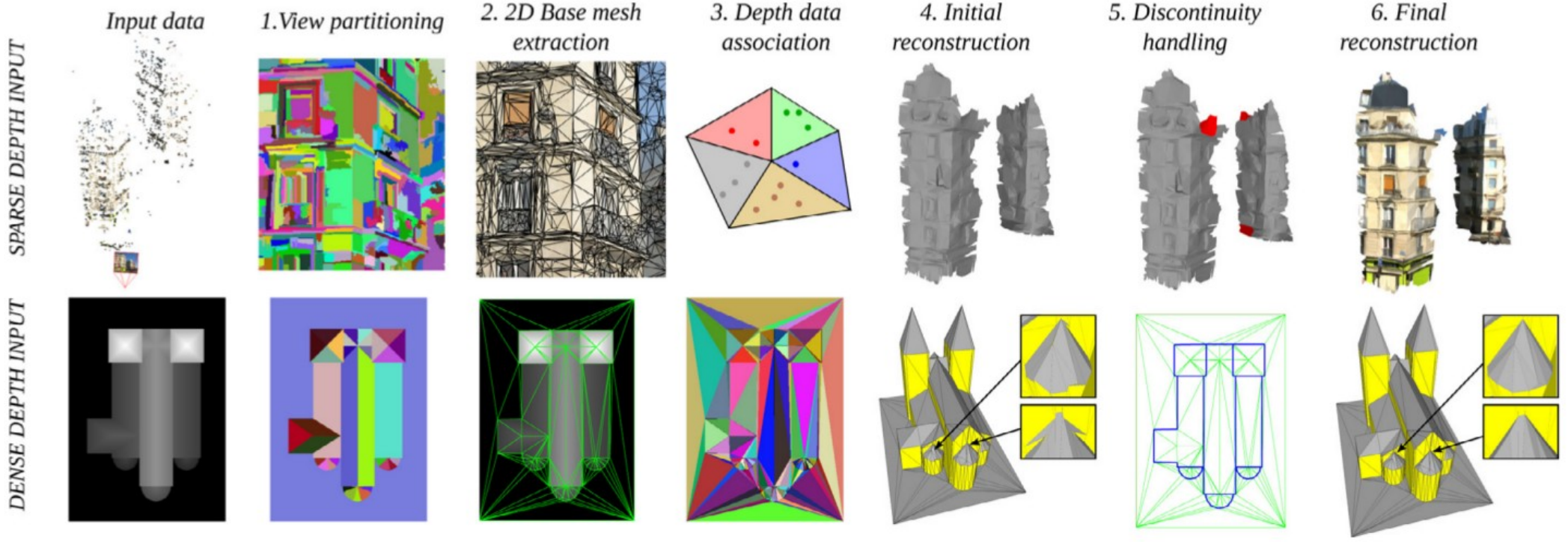

LG2 – Architectural Decomposition for 3D Landmark Building Understanding

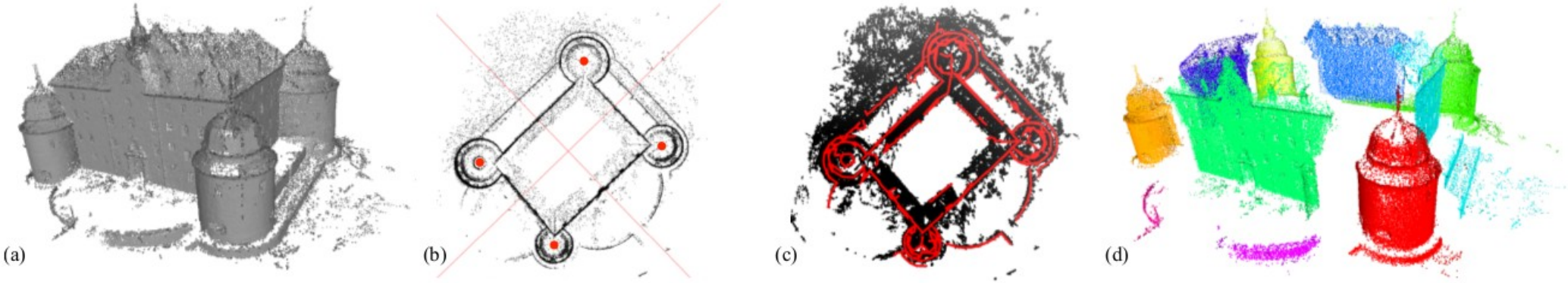

OT1 – Adaptive Sparse Representation for Analyzing Artistic Style of Paintings

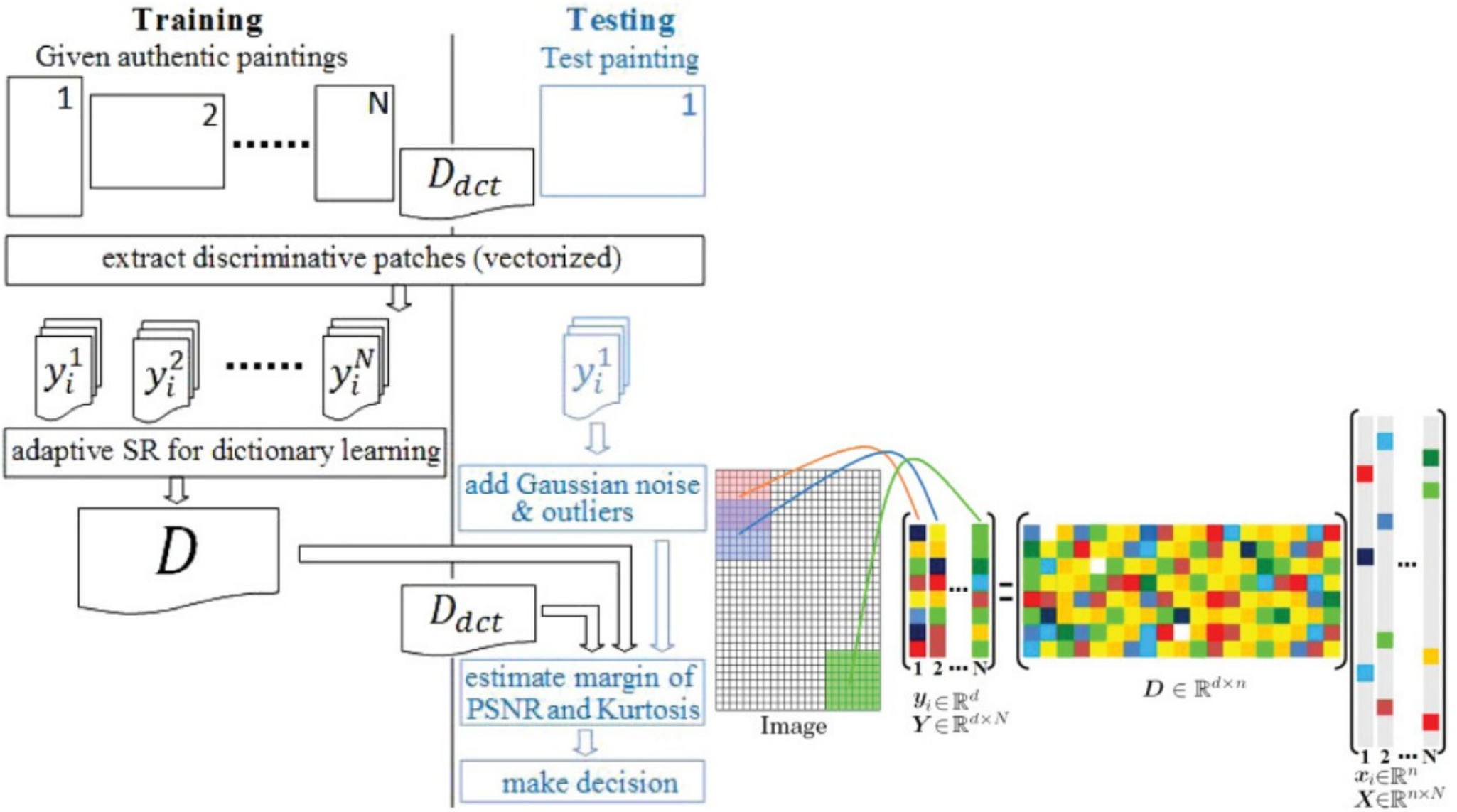

OT2 – 3D Artifacts Similarity Based on the Concurrent Evaluation of Heterogeneous Properties

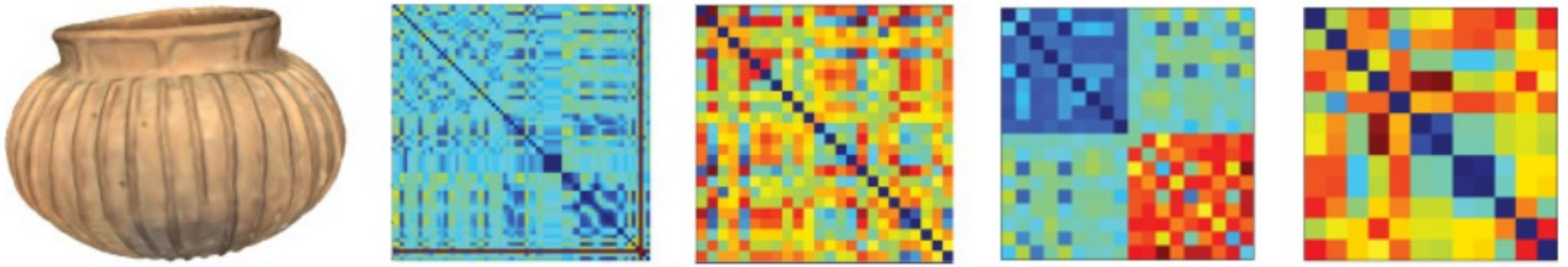

(a) (b) (c) (d) (e)

Fig. 2. A model from the dataset (*a*) and the corresponding MDM signature with 70, 26, 18, and 12 functions (*b*–*e*). The distances range from blue (0) to red (1); large blue regions indicate functions that are strongly similar.

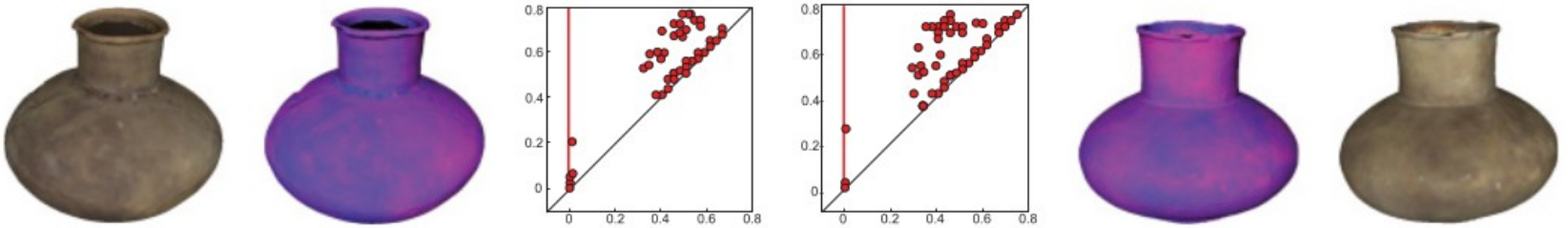

(a) (b) (c) (d) (e) (f)

OT3 – Partial 3D Object Retrieval combining Local Shape Descriptors with Global Fisher Vectors

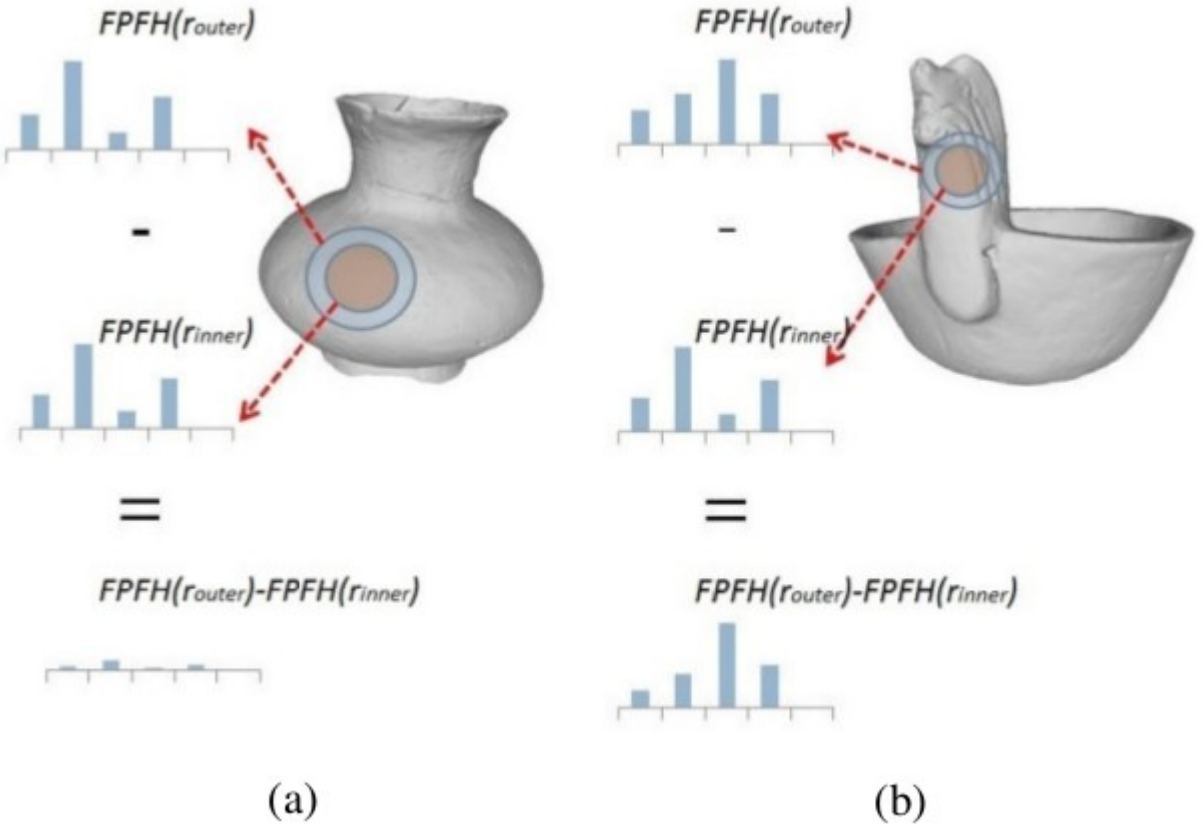

RS1 – Batched Dynamic Adaptive Meshes for High Performance Terrain Visualization

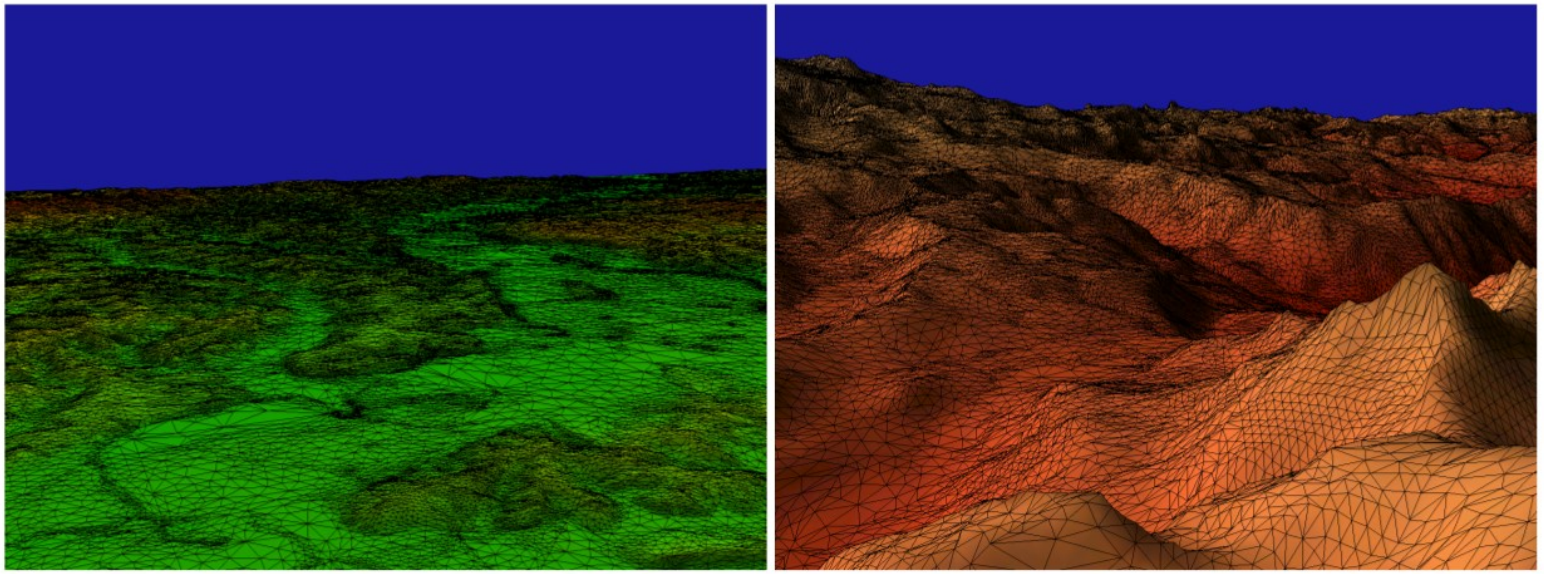

(a) Frame 400 (b) Frame 1751

Figure 10: ***Selected flythrough frames.*** *Screen space error tolerance set to 1.0 pixels.*

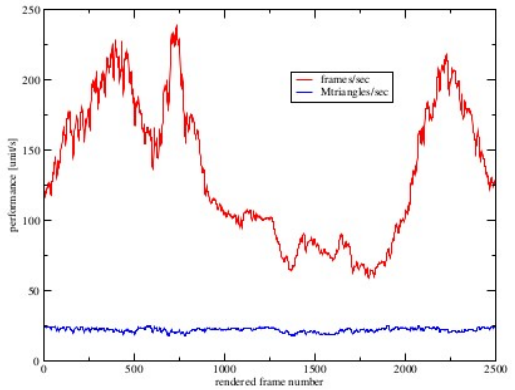

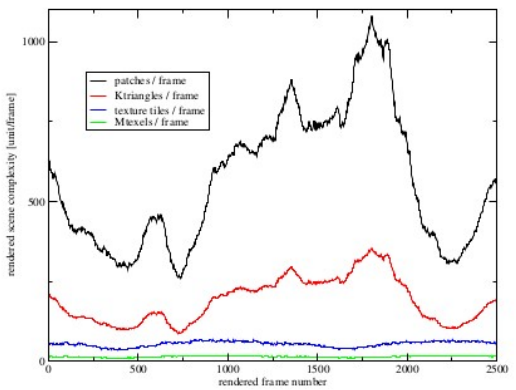

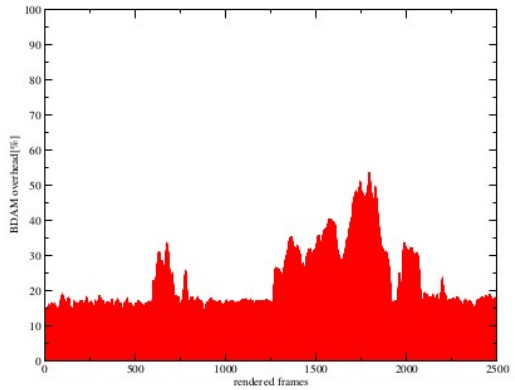

RS2a – Multiple Texture Stitching and Blending on 3D Objects

Fig. 8. On the left are shown (rendered wire-frame) the faces of M which are linked to a particular input image; in this case the corresponding texture section has an elongated shape, which can cause some space overhead in the final texture T_M (shown on the right).

RS2b – Masked photo blending: mapping dense photographic data set on high-resolution sampled 3D models

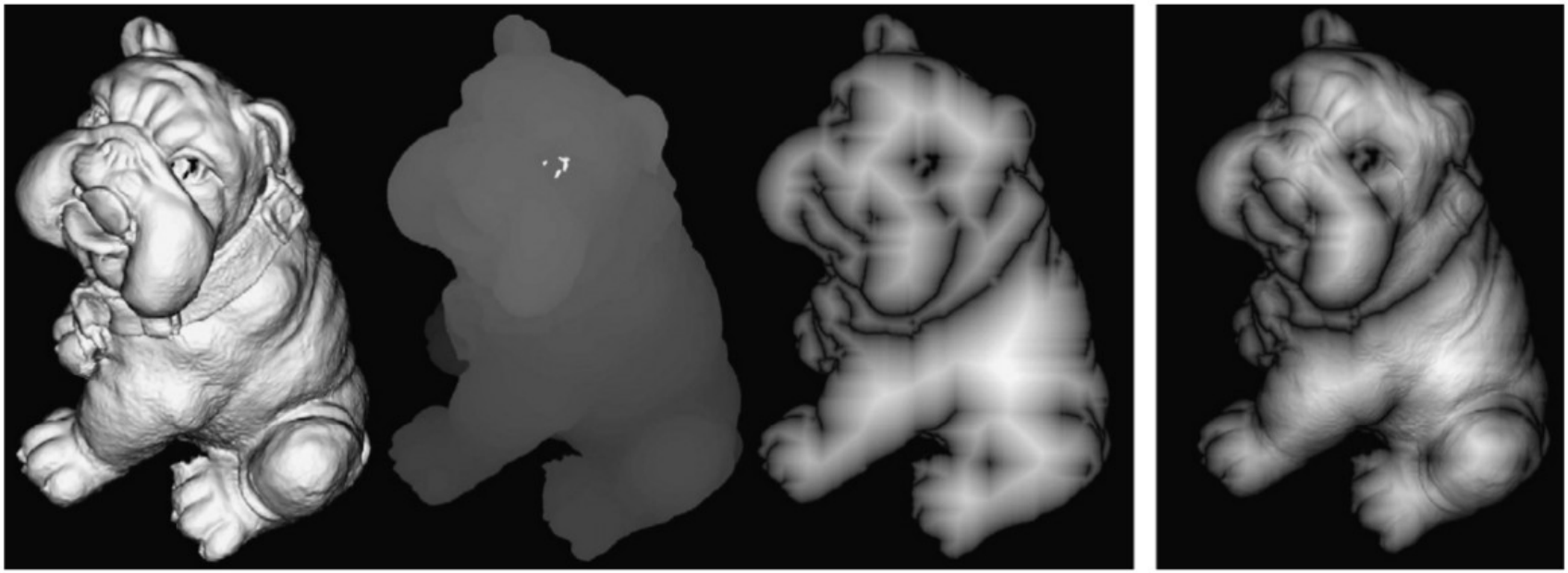

Fig. 2. An example of the core weighting masks. From left to right: angle Mask, depth mask and border mask. Rightmost, all the masks combined in the final mask. Caveat: the contrast of the depth and border masks has been increased for enhanced readability.

RS3 – Archeological excavation monitoring using dense stereo matching techniques

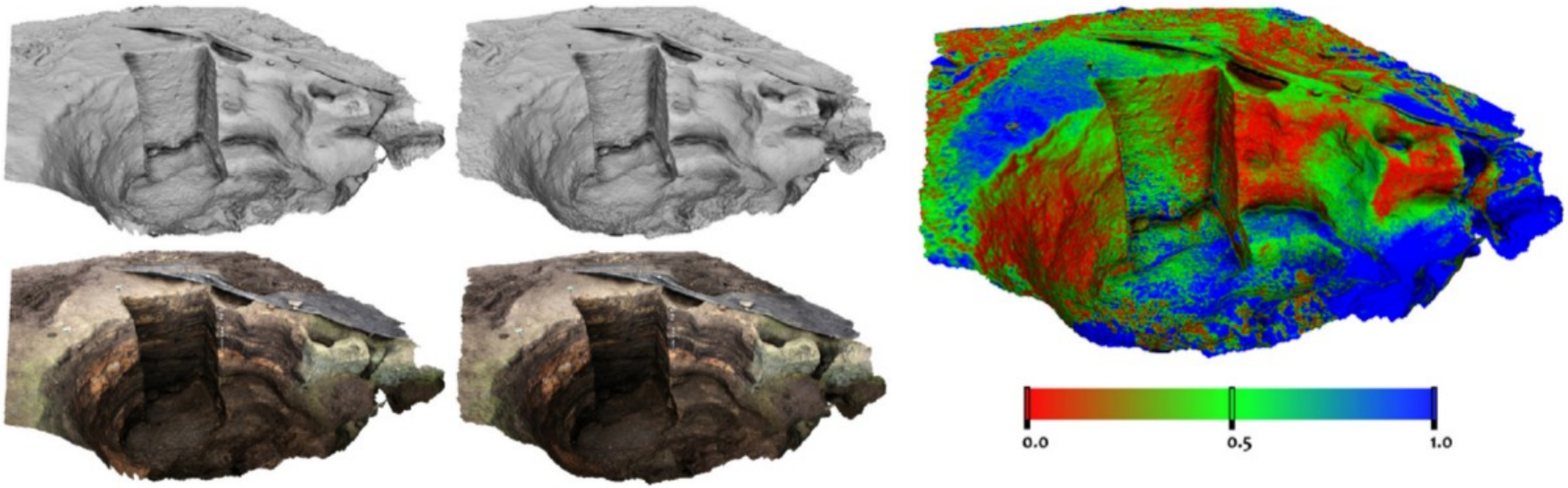

Fig. 3. Repeatability Test. Left: the two datasets of the same object (pure geometry above and with mapped color below). It is possible to appreciate their really similar appearance. Right: the color-coded deviation between the two models; 90% of the model is below 1 cm deviation. Reference color scale is shown below the model (unit is in cm).

RS4 – Simplification of Tetrahedral Meshes with Accurate Error Evaluation

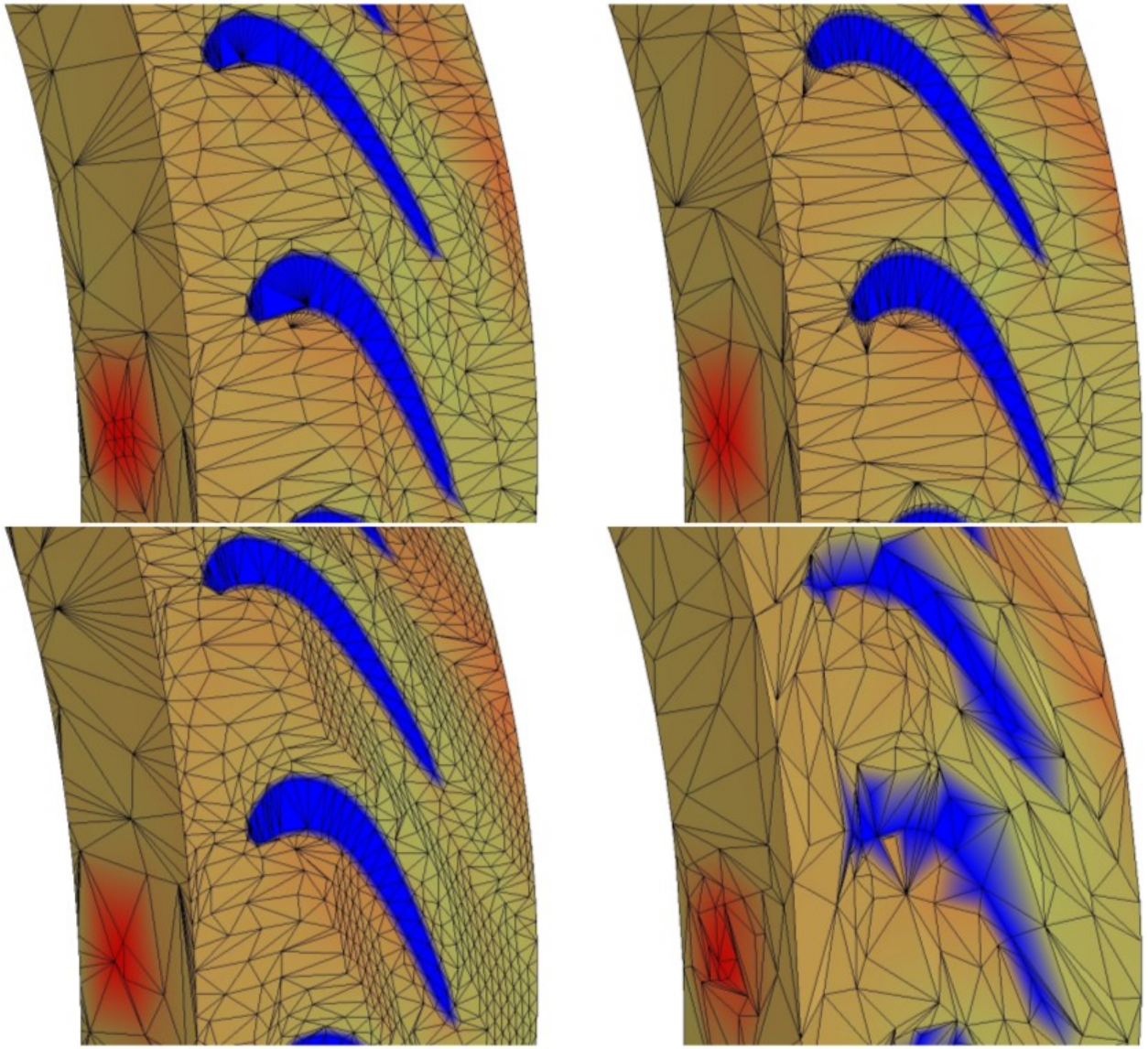

Figure 4: Different simplified meshes produced from the Turbine Blade dataset. The different meshes shown, of size 10,679 vertices, were produced with the **BF**, **BFS**, **LN** and **QD** techniques (from top-left, clockwise).

RS5 – Field Aligned Mesh Joinery

Fig. 1. Given a 3D shape with a smooth cross-field, we generate a set of planar slices that can be interlocked in a self supporting structure.

(a) (b) (c)

SH1 – Generating Semantic 3D Models of Underground Infrastructure

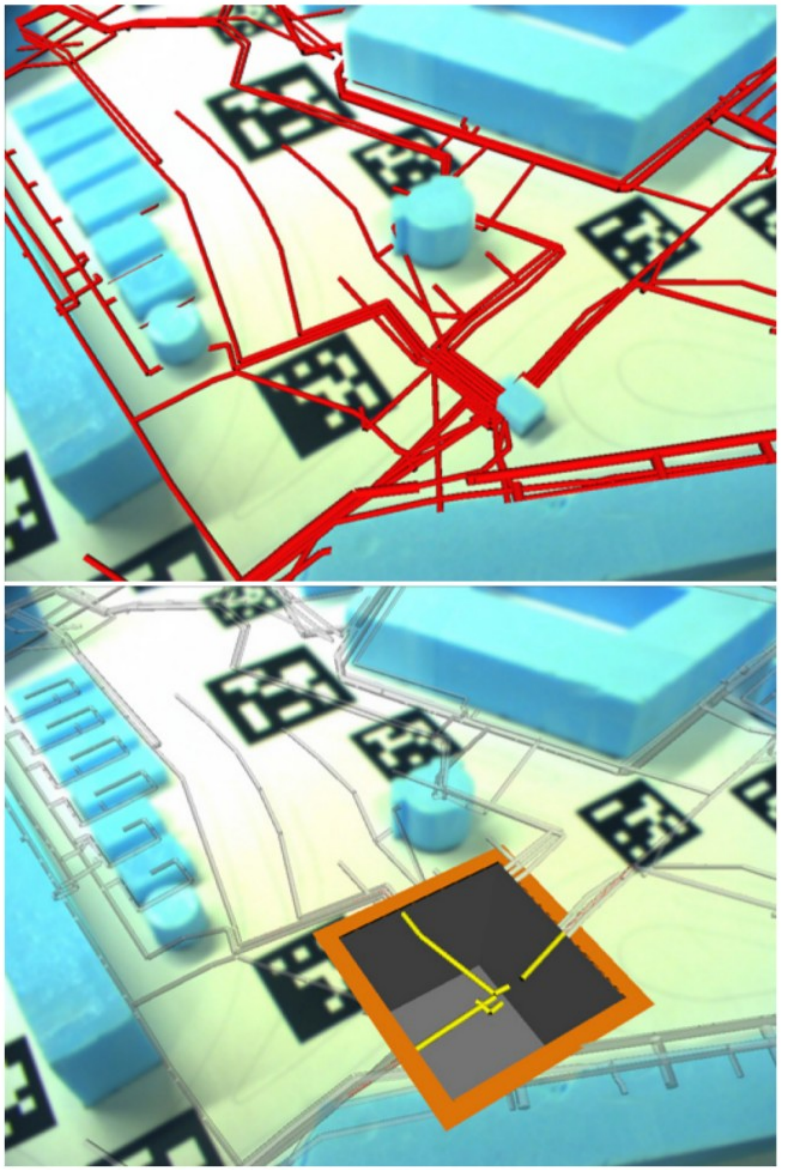

SH2 – Generative Parametric Design of Gothic Window Tracery

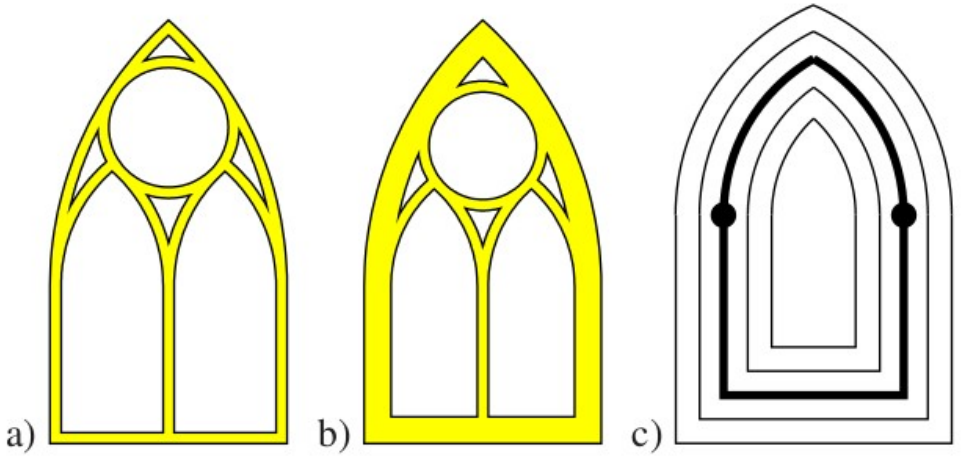

Figure 7: *a),b) The regions are shrunk to embed them in a common border plane. c) The offset operation changes the excess of a pointed arch, but keeps the circle midpoints constant.*

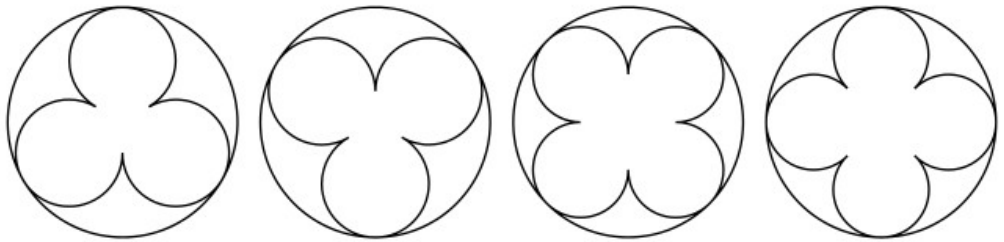

Figure 8: *Lying and standing trefoil and quatrefoil rosettes.*

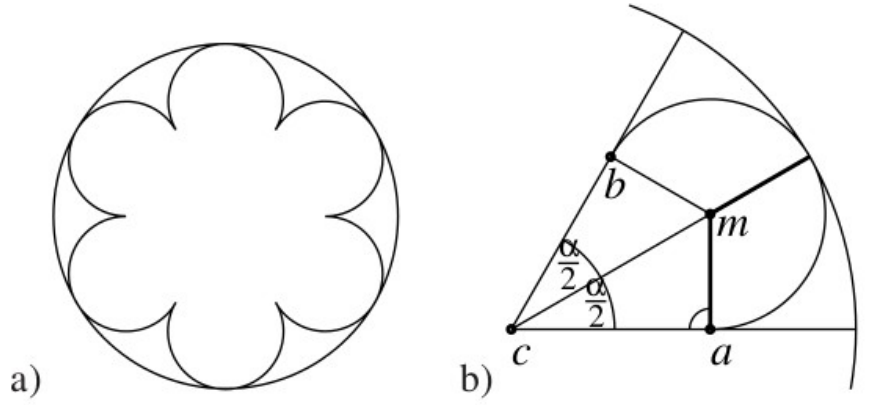

Figure 9: *Construction of a rosette with six rounded foils, so* $\alpha = \frac{2\pi}{6}$.

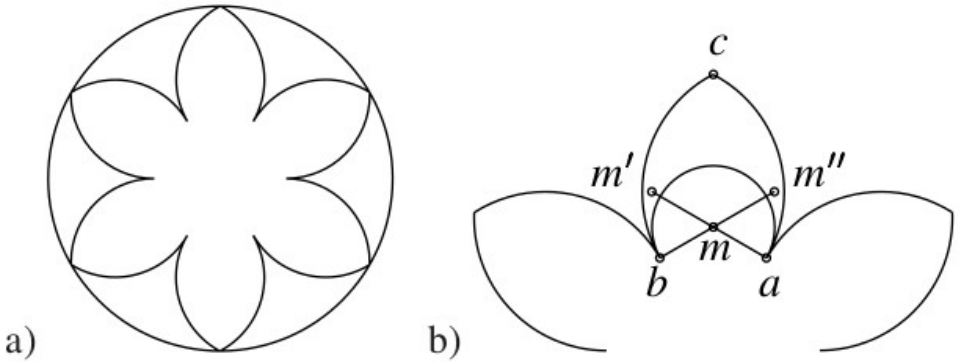

Figure 10: *Construction of a rosette with pointed foils, with a relative displacement of 1.15 to obtain* m' *and* m'' *from m.*

SH3 – Shape grammars on convex polyhedra